Hybrid-Ring Directional Coupler for Arbitrary Power Divisions*

CHUCK Y. PON†, MEMBER, IRE

Summary—A directional coupler in the form of a hybrid ring is described in this paper. A theoretical analysis using the scattering matrix has been carried out and experimental verification of the theoretical result has been achieved in a stripline network.

Simple design equations which enable one to design a directional coupler with any degree of coupling have been derived. This coupler differs from the commonly used couplers in that the voltages at the output arms are either in-phase or opposite-phase with respect to each other. In addition, its geometrical symmetry makes it very convenient for use in symmetrical networks, particularly as a power divider in antenna feeding systems.

Introduction

THE important common properties possessed by all directional couplers are: 1) the output arms are isolated from each other, and 2) the input impedance is matched looking into any arm when the other arms are terminated by match impedances.

Since the conventional simple Y-junction power dividers do not possess these properties, directional couplers are preferable for certain applications, such as antenna array feed systems where the need for minimizing mutual coupling puts a premium on isolation between the output arms of the power dividers. The inherent match of the directional coupler compensates for its larger size in that the matching transformers necessary with the Y junction are not required.

The two-dimensional structure of stripline facilitates the construction of numerous directional couplers which have found extensive applications in microwave circuits. Among the various types of stripline directional couplers, the ones which are most commonly used and easiest to construct are the quarter-wave parallel-line couplers and the quarter-wave branch-line couplers shown in Fig. 1. The theoretical analyses and the design equations for these couplers have been discussed extensively in the literature.[1-3] For particular applications significant factors that must be considered are physical configuration and the inherent 90° phase difference between the output arms.

* Received by the PGMTT, May 8, 1961; revised manuscript received, July 24, 1961.

† Dalmo Victor Co., Div. of Textron, Inc., Belmont, Calif.

[1] S. B. Cohn, P. M. Sherk, J. K. Shimizu, E. M. T. Jones, "Strip Transmission Lines and Components," Stanford Research Institute, Menlo Park, Calif., Final Rept., Contract DA 36-039-SC 73232 DA, pp. 45–77; February, 1957.

[2] Leo Young, "Branch guide directional couplers," *Proc. Natl. Electronics Conf.*, Chicago, Ill., October 1–3, 1956; National Electronics Conference, Inc., Chicago, Ill., vol. 12, pp. 723–732, April 15, 1957.

[3] J. Reed and G. J. Wheeler, "A method of analysis of symmetrical four-port networks," IRE TRANS. ON MICROWAVE THEORY AND TECHNIQUES, vol. MTT-4, pp. 246–252; October, 1956.

The directional coupler described in this paper has the configuration of a hybrid ring (Fig. 2). The important features of this coupler are:

1) The input impedance is matched to the characteristic impedance of any arm when its two adjacent arms are terminated by matched loads.
2) The two output arms are isolated from each other.
3) The voltages in the two output arms are either in-phase or 180° out of phase, depending on the input arms chosen.
4) The power-split ratio is adjusted by varying the impedances between the arms.

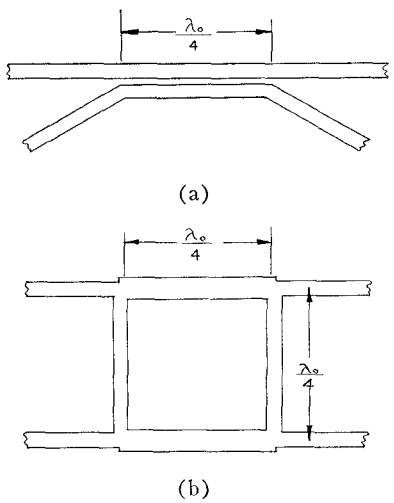

Fig. 1—(a) Parallel-line directional coupler. (b) Branch-line directional coupler.

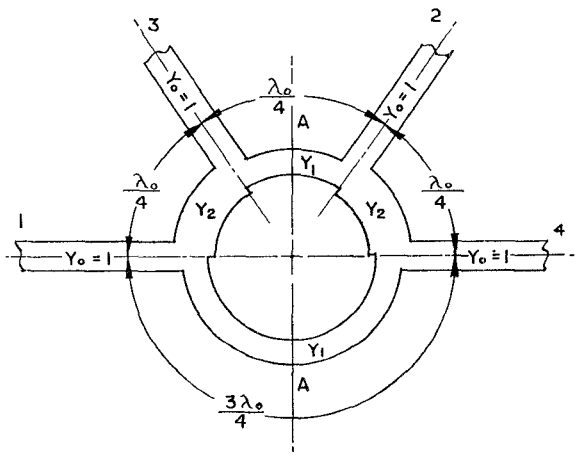

Fig. 2—Hybrid-ring directional coupler.

The relative advantage of each directional coupler described above depends on the physical arrangement and the desired electrical characteristics of the circuit in which it is to be incorporated. For instance, in an equiphase, symmetrical, parallel-feed antenna array, the hybrid-ring directional coupler has a definite advantage over the parallel-line and branch-line couplers because no phase-compensating element is necessary for the former. Also, the hybrid-ring coupler has broader bandwidth than does the branch-line coupler.

Analysis of the Hybrid-Ring Directional Coupler

A general configuration of a hybrid-ring directional coupler is illustrated in Fig. 2. The characteristic admittances of the four arms are equal and normalized. The variable parameters are the two admittances Y_1 and Y_2, which determine the degree of coupling of the output arms and the impedance matching condition for the input arm.

The analysis of this hybrid-ring coupler consists of the usual procedure of reducing the four-terminal network to a two-terminal network by taking advantage of the symmetry about the plane A-A. For example, when two in-phase waves of unit amplitude are applied to terminals 1 and 4, or to terminals 2 and 3, the current is zero at the plane A-A. As a result, the ring can be open-circuited at this plane and only one half of the circuit needs to be analyzed. This condition is called the even mode and all the parameters associated with this mode are denoted by the subscript e (Fig. 3). When two opposite-phase waves of unit amplitude are applied to terminals 1 and 4, or to terminals 2 and 3, the voltage is zero at the plane A-A. As a result, the ring can be short-circuited at this plane and, again, only one half of the circuit needs to be analyzed. This condition is called the odd mode and all parameters associated with this mode are identified by the subscript o (Fig. 4).

The equivalent circuits for these two modes are also shown in their respective figures. The incident and reflected waves are denoted as a and b, respectively.

Once the scattering matrices for the even and odd modes are known, the reflected waves in each arm can be determined. Then, by superimposing the waves of the two modes, we have the resultant reflected waves in each arm and a single incident wave in one arm.

To find the scattering matrix for each mode, we first derive the admittance matrix for each mode. From Fig. 3(d), we find that the admittance matrix for the even mode is

$$[Y]_e = j\begin{bmatrix} -Y_1 & Y_2 \\ Y_2 & Y_1 \end{bmatrix}. \tag{1}$$

From Figure 4(d), the admittance matrix for the odd mode is

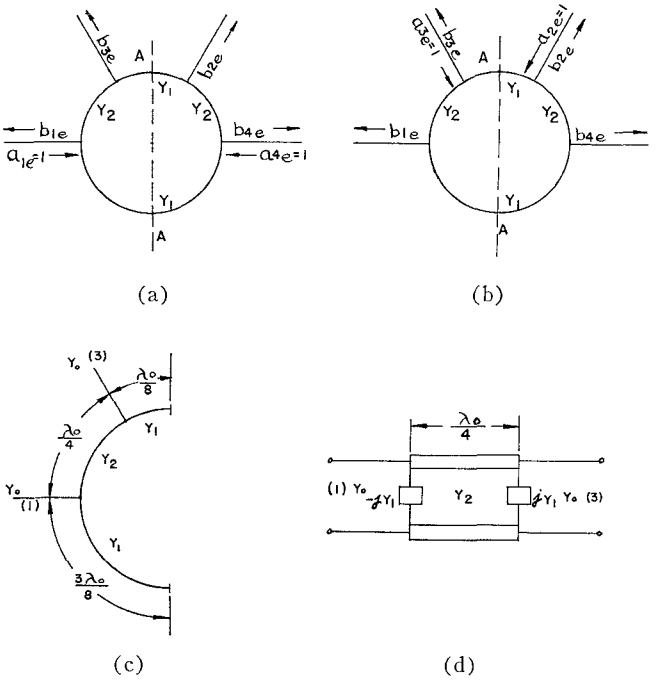

Fig. 3—(a) Incident waves at arms 1 and 4. (b) Incident waves at arms 2 and 3. (c) Open circuit at A-A. (d) Equivalent circuit.

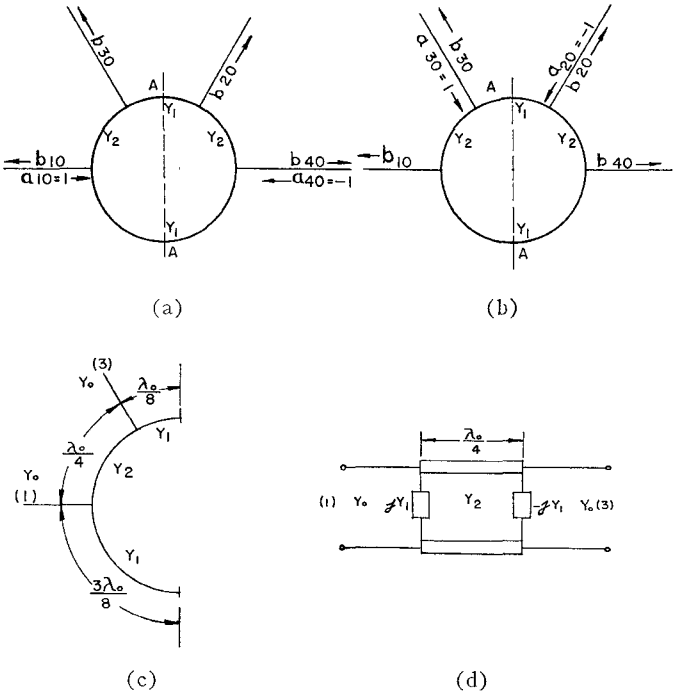

Fig. 4—Odd mode. (a) Incident waves at arms 1 and 4. (b) Incident waves at arms 2 and 3. (c) Short circuit at A-A. (d) Equivalent circuit.

$$[Y]_o = j\begin{bmatrix} Y_1 & Y_2 \\ Y_2 & -Y_1 \end{bmatrix}. \tag{2}$$

The scattering matrix is related to the admittance matrix by

$$[S] = [I - Y][I + Y]^{-1}. \tag{3}$$

Carrying out the matrix operations, we have for the even-mode scattering matrix

$$[S]_e = \begin{bmatrix} \dfrac{1 - Y_1^2 - Y_2^2 + j2Y_1}{1 + Y_1^2 + Y_2^2} & \dfrac{-j2Y_2}{1 + Y_1^2 + Y_2^2} \\ \dfrac{-j2Y_2}{1 + Y_1^2 + Y_2^2} & \dfrac{1 - Y_1^2 - Y_2^2 - j2Y_1}{1 + Y_1^2 + Y_2^2} \end{bmatrix}, \tag{4}$$

and for the odd-mode scattering matrix

$$[S]_o = \begin{bmatrix} \dfrac{1 - Y_1^2 - Y_2^2 - j2Y_1}{1 + Y_1^2 + Y_2^2} & \dfrac{-j2Y_2}{1 + Y_1^2 + Y_2^2} \\ \dfrac{-j2Y_2}{1 + Y_1^2 + Y_2^2} & \dfrac{1 - Y_1^2 - Y_2^2 + j2Y_1}{1 + Y_1^2 + Y_2^2} \end{bmatrix}. \tag{5}$$

Recalling that the reflected waves are related to the incident wave by

$$[b] = [S][a], \tag{6}$$

we can now determine the reflected wave in each arm for each mode. Thus, for the first case in which the incident waves are at arms 1 and 4, the reflected waves for the even mode are

$$b_{1e} = b_{4e} = \frac{1 - Y_1^2 - Y_2^2 + j2Y_1}{1 + Y_1^2 + Y_2^2} \tag{7}$$

$$b_{2e} = b_{3e} = \frac{-j2Y_2}{1 + Y_1^2 + Y_2^2}, \tag{8}$$

and for the odd mode are

$$b_{1o} = -b_{4o} = \frac{1 - Y_1^2 - Y_2^2 - 2jY_1}{1 + Y_1^2 + Y_2^2} \tag{9}$$

$$b_{2o} = -b_{3o} = \frac{j2Y_2}{1 + Y_1^2 + Y_2^2}. \tag{10}$$

The resultant waves when the even and odd modes are superimposed are

$$a_1 = 2 \tag{11}$$

$$b_1 = 2\left(\frac{1 - Y_1^2 - Y_2^2}{1 + Y_1^2 + Y_2^2}\right) \tag{12}$$

$$b_2 = 0 \tag{13}$$

$$b_3 = \frac{-j4Y_2}{1 + Y_1^2 + Y_2^2} \tag{14}$$

$$b_4 = \frac{j4Y_1}{1 + Y_1^2 + Y_2^2}. \tag{15}$$

Similarly, for the second case in which the incident waves are at arms 2 and 3, the reflected waves for the even mode are

$$b_{1e} = b_{4e} = \frac{-j2Y_2}{1 + Y_1^2 + Y_2^2} \tag{16}$$

$$b_{2e} = b_{3e} = \frac{1 - Y_1^2 - Y_2^2 - j2Y_1}{1 + Y_1^2 + Y_2^2}, \tag{17}$$

and for the odd mode are

$$b_{1o} = -b_{4o} = \frac{-2jY_2}{1 + Y_1^2 + Y_2^2} \tag{18}$$

$$b_{2o} = -b_{3o} = -\left(\frac{1 - Y_1^2 - Y_2^2 - j2Y_1}{1 + Y_1^2 + Y_2^2}\right). \tag{19}$$

The resultant waves when the even and odd modes are superimposed are

$$a_3 = 2 \tag{20}$$

$$b_1 = \frac{-j4Y_2}{1 + Y_1^2 + Y_2^2} \tag{21}$$

$$b_2 = \frac{-j4Y_1}{1 + Y_1^2 + Y_2^2} \tag{22}$$

$$b_3 = 2\left(\frac{1 - Y_1^2 - Y_2^2}{1 + Y_1^2 + Y_2^2}\right). \tag{23}$$

The condition that the input arm in both cases be perfectly matched requires that b_1 in (12) and b_3 in (23) be zero, from which we get

$$Y_1^2 + Y_2^2 = 1. \tag{24}$$

The resultant waves for the two cases are summarized in Figs. 5(a) and 5(b). The output voltage ratio between arms 3 and 4 in Fig. 5(a) is

$$\frac{b_3}{b_4} = -\frac{Y_2}{Y_1}, \tag{25}$$

and the output voltage ratio between arms 1 and 2 in Fig. 5(b) is

$$\frac{b_1}{b_2} = \frac{Y_2}{Y_1}. \tag{26}$$

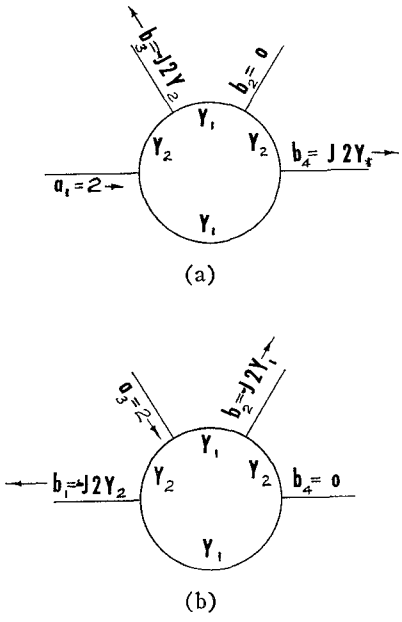

Fig. 5—Incident and reflected waves.

Eq. (25) states that for an input voltage at arm 1 the output voltages at arms 3 and 4 are 180° out of phase. Eq. (26) states that for an input voltage at arm 3, the output voltages at arms 1 and 2 are in-phase.

From the last three equations, one can design a matched power divider with any desired power ratio by using the proper admittances Y_1 and Y_2. It can be observed that for equal power split, *i.e.*, $P_3/P_4 = 1$, Y_1 and Y_2 are equal to $1/\sqrt{2}$, which is recognized as the admittance for the well-known 3-db "rat race" ring.

Finally, the scattering matrix characterizing this directional coupler can be written as

$$[S] = \begin{bmatrix} 0 & 0 & -jY_2 & jY_1 \\ 0 & 0 & -jY_1 & -jY_2 \\ -jY_2 & -jY_1 & 0 & 0 \\ jY_1 & -jY_2 & 0 & 0 \end{bmatrix}. \qquad (27)$$

The results obtained above are for a single frequency. To find the frequency dependence of this hybrid-ring coupler, it is necessary to use the equivalent circuits and derivations as given in the Appendix. The power emerging from each arm relative to the input power at arm 1 and the input VSWR as a function of frequency for a 3-db and a 10-db power split are plotted in Figs. 6(a) and 6(b), respectively. For comparison, the isolation and VSWR for a branch-line 3-db power split is also plotted on Fig. 6(a), from which we can see that the hybrid-ring coupler has broader bandwidth than the branch-line coupler. Due to the lack of available data on the parallel-line coupler, no comparison can be made with it at this time.

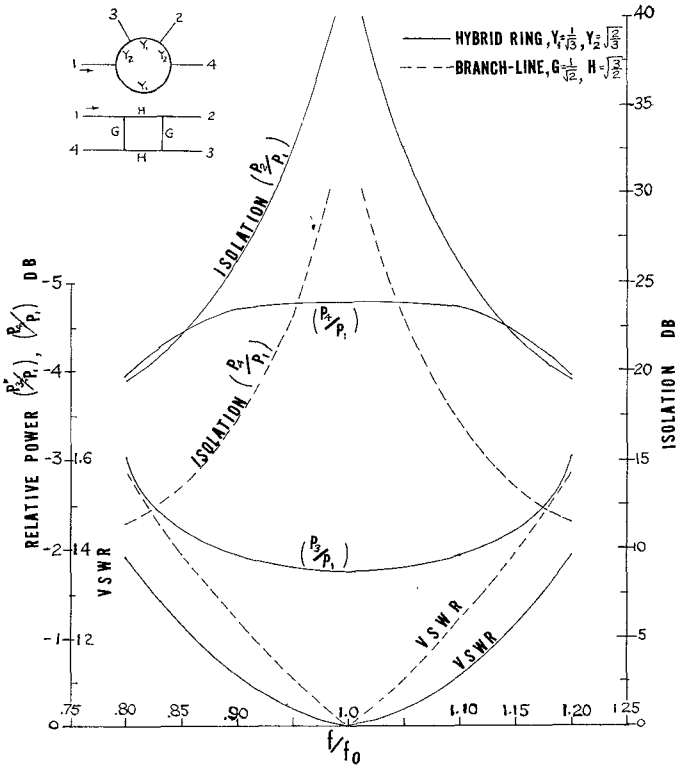

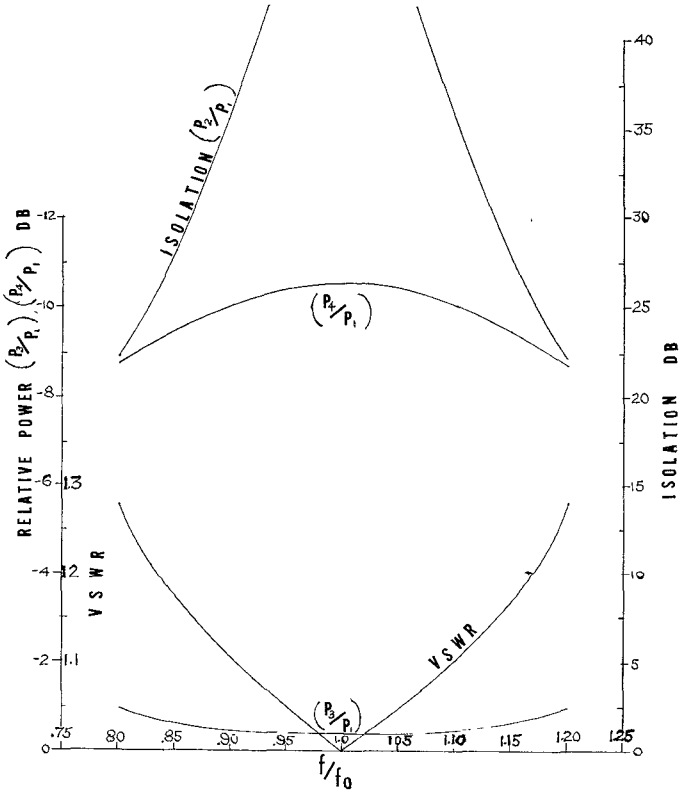

Fig. 6—(a) Relative power and VSWR for 3-db power split. (b) Relative power and VSWR for 10-db power split.

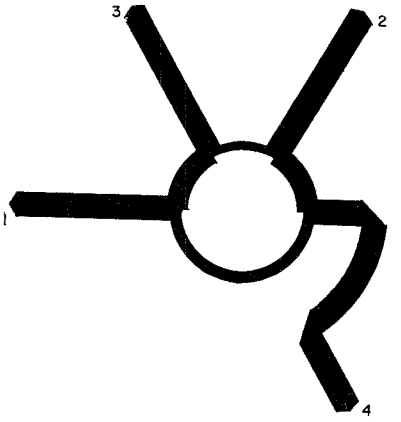

Fig. 7—2.5:1 Stripline power divider.

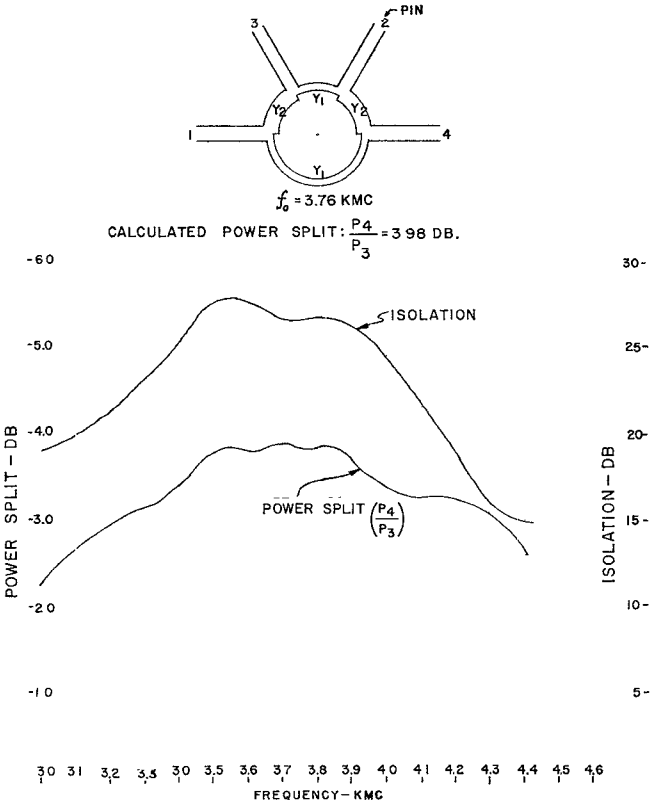

Fig. 8—Power split and isolation of hybrid-ring coupler.

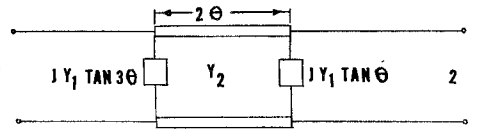

$$\theta = \frac{\pi}{4} \frac{\lambda_0}{\lambda}$$

Fig. 9—Equivalent circuit for one-half of the ring circuit for the even mode.

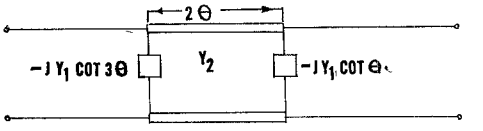

Fig. 10—Equivalent circuit for one-half of the ring circuit for the odd mode.

Experimental Results

A stripline hybrid-ring directional coupler with a power split ratio of 3.98 db between the two output arms at the center frequency of 3.76 kMc was designed and tested. The configuration of this power divider is shown in Fig. 7. The measured power split and isolation are shown in Fig. 8. Close agreement is observed between measured and calculated values. The results obtained in this analysis are valid for any type of transmission line in which a T can be constructed. It might be worthwhile to point out another advantage of using the hybrid-ring coupler as a power divider in place of a Y-junction power divider. Generally, the power-split ratio of a power divider is controlled by varying some characteristic admittances, the allowable values of which are limited by constructional tolerances, in the circuit. For a Y junction, the power-split ratio is proportional to the admittance ratio between its output arms. For a hybrid-ring coupler, the power-split ratio is proportional to the square of the admittance ratio of the two variable admittances in the ring. Therefore, the maximum attainable power split in any transmission line is greater for the hybrid-ring coupler than for the Y-junction power divider.

Appendix

Admittance Matrix for the Even Mode

$$Y_{11e} = j(Y_1 \tan 3\theta - Y_2 \cot 2\theta) \tag{28}$$

$$Y_{22e} = j(Y_1 \tan \theta - Y_2 \cot 2\theta) \tag{29}$$

$$Y_{12e} = Y_{21e} = jY_2 \csc 2\theta. \tag{30}$$

Admittance Matrix for the Odd Mode

$$Y_{11o} = -j(Y_1 \cot 3\theta + Y_2 \cot 2\theta) \tag{31}$$

$$Y_{22o} = -j(Y_1 \cot \theta + Y_2 \cot 2\theta) \tag{32}$$

$$Y_{12o} = Y_{21o} = jY_2 \csc 2\theta \tag{33}$$

Scattering Matrix

$$[S] = [I - Y][I + Y]^{-1} = \begin{bmatrix} \dfrac{1 - Y_{11} + Y_{22} - Y_{11}Y_{22} + Y_{12}^2}{1 + Y_{11} + Y_{22} + Y_{11}Y_{22} - Y_{12}^2} & \dfrac{-2Y_{12}}{1 + Y_{11} + Y_{22} + Y_{11}Y_{22} - Y_{12}^2} \\ \dfrac{-2Y_{12}}{1 + Y_{11} + Y_{22} + Y_{11}Y_{22} - Y_{12}^2} & \dfrac{1 + Y_{11} - Y_{22} - Y_{11}Y_{22} + Y_{12}^2}{1 + Y_{11} + Y_{22} + Y_{11}Y_{22} - Y_{12}^2} \end{bmatrix}. \tag{34}$$

1) *For the Even Mode:*

$$[S]_e = \begin{bmatrix} S_{11e} & S_{12e} \\ S_{21e} & S_{22e} \end{bmatrix}. \tag{35}$$

Substituting (28)–(30) into (34), we get

$$S_{11e} = \frac{1 - Y_2^2 + Y_1^2 \tan 3\theta \tan\theta - Y_1Y_2 \cot 2\theta(\tan 3\theta + \tan\theta) + jY_1(\tan\theta - \tan 3\theta)}{1 + Y_2^2 - Y_1^2 \tan 3\theta \tan\theta + Y_1Y_2 \cot 2\theta(\tan 3\theta + \tan\theta) + j[Y_1(\tan 3\theta + \tan\theta) - 2Y_2 \cot 2\theta]} \tag{36}$$

$$S_{12e} = S_{21e} = \frac{-j2Y_2 \csc 2\theta}{1 + Y_2^2 - Y_1^2 \tan 3\theta \tan\theta + Y_1Y_2 \cot 2\theta(\tan 3\theta + \tan\theta) + j[Y_1(\tan 3\theta + \tan\theta) - 2Y_2 \cot 2\theta]} \tag{37}$$

$$S_{22e} = \frac{1 - Y_2^2 + Y_1^2 \tan 3\theta \tan\theta - Y_1Y_2 \cot 2\theta(\tan 3\theta + \tan\theta) + jY_1(\tan 3\theta - \tan\theta)}{1 + Y_2^2 - Y_1^2 \tan 3\theta \tan\theta + Y_1Y_2 \cot 2\theta(\tan 3\theta + \tan\theta) + j[Y_1(\tan 3\theta + \tan\theta) - 2Y_2 \cot 2\theta]}. \tag{38}$$

2) *For the Odd Mode:*

$$[S]_0 = \begin{bmatrix} S_{11o} & S_{12o} \\ S_{21o} & S_{22o} \end{bmatrix}. \tag{39}$$

Substituting (31)–(33) into (34), we get

$$S_{11o} = \frac{1 - Y_2^2 + Y_1^2 \cot 3\theta \cot\theta + Y_1Y_2 \cot 2\theta(\cot 3\theta + \cot\theta) - jY_1(\cot\theta - \cot 3\theta)}{1 + Y_2^2 - Y_1^2 \cot 3\theta \cot\theta - Y_1Y_2 \cot 2\theta(\cot 3\theta + \cot\theta) - j[Y_1(\cot 3\theta + \cot\theta) + 2Y_2 \cot 2\theta]} \tag{40}$$

$$S_{12o} = S_{21o} = \frac{-j2Y_2 \csc 2\theta}{1 + Y_2^2 - Y_1^2 \cot 3\theta \cot\theta - Y_1Y_2 \cot 2\theta(\cot 3\theta + \cot\theta) - j[Y_1(\cot 3\theta + \cot\theta) + 2Y_2 \cot 2\theta]} \tag{41}$$

$$S_{22o} = \frac{1 - Y_2^2 + Y_1^2 \cot 3\theta \cot\theta + Y_1Y_2 \cot 2\theta(\cot 3\theta + \cot\theta) - jY_1(\cot 3\theta - \cot\theta)}{1 + Y_2^2 - Y_1^2 \cot 3\theta \cot\theta - Y_1Y_2 \cot 2\theta(\cot 3\theta + \cot\theta) - j[Y_1(\cot 3\theta + \cot\theta) + 2Y_2 \cot 2\theta]}. \tag{42}$$

For two in-phase waves of unit amplitude incident on arms 1 and 4, the reflected waves for the even mode are

$$a_1 = 1, \qquad a_4 = 1 \tag{43}$$

$$b_{1e} = b_{4e} = S_{11e} \tag{44}$$

$$b_{2e} = b_{3e} = S_{12e}. \tag{45}$$

For two opposite-phase waves of unit amplitude incident on arms 1 and 4, the reflected waves for the odd mode are

$$b_{1o} = -b_{4o} = S_{11o} \tag{46}$$

$$b_{3o} = -b_{2o} = S_{12o}. \tag{47}$$

Adding the even and odd modes together, we have the resultant incident and reflected waves

$$a_1 = 2 \tag{48}$$

$$b_1 = b_{1e} + b_{1o} = S_{11e} + S_{11o} \tag{49}$$

$$b_2 = b_{2e} + b_{2o} = S_{12e} - S_{12o} \tag{50}$$

$$b_3 = b_{3e} + b_{3o} = S_{12e} + S_{12o} \tag{51}$$

$$b_4 = b_{4e} + b_{4o} = S_{11e} - S_{11o}. \tag{52}$$

Similarly, for waves incident on arms 2 and 3, we have for the resultant incident and reflected waves

$$a_3 = 2 \tag{53}$$

$$b_1 = S_{12e} + S_{12o} \tag{54}$$

$$b_2 = S_{22e} - S_{22o} \tag{55}$$

$$b_3 = S_{22e} + S_{22o} \tag{56}$$

$$b_4 = S_{12e} - S_{12o}. \tag{57}$$

ACKNOWLEDGMENT

The author wishes to acknowledge Dr. J. Carpenter, F. Hennessey and A. B. Hadik-Barkóczy for their helpful suggestions concerning this paper.

A Coupled Strip-Line Configuration Using Printed-Circuit Construction that Allows Very Close Coupling*

WILLIAM J. GETSINGER†, MEMBER, IRE

Summary—A new strrip-line configuration is presented, applicable to printed-circuit construction, that allows very close coupling to be achieved without esorting to very small coupling gaps and excessively critical dimensions. Graphs of even- and odd-mode fringing capacitances are given. These graphs can be used with simple formulas, which also are given, to determine the dimensions of the configuration that will give specified even- and odd-mode characteristic impedances or shunt capacitances.

The usefulness of the graphs and formulas was demonstrated by using them to design 3-db backward-couplers. The performance of the couplers in this new configuration was typical of similar couplers made in more conventional configurations, as expected. However, the devices shown have an advantage in that they can be manufactured by relatively inexpensive and rapid printed-circuit methods and, since the region between the conductors is solid dielectric, they are unusually rugged.

I. GENERAL

IN working with shielded strip-line, the need for closely coupled strips arises in designing 3-db couplers [1] and broad-band filters [2], [3]. The typical printed-circuit coupled strip-line configuration consists of two slabs of dielectric sandwiched between parallel ground planes. One of the slabs has two parallel copper strips printed on it. Coupling is achieved by bringing adjacent edges of the two strips close enough to cause appreciable capacitance to exist between the strips. Very close coupling requires that the strips be brought very near each other. For the 3-db coupler, and even more for very broad-band parallel-coupled filters, the spacing between strips becomes too small to be made accurately using practical construction techniques because the allowable tolerance on the spacing decreases as the spacing decreases. Thus, there is a practical limit to the inter-strip capacitance that can be achieved with edge-coupled thin strips.

One solution to this problem has been to orient the coupled strips face-to-face and perpendicular to the ground planes. While this achieves large inter-strip capacitance, it is not always a desirable configuration, because it is difficult to build and it does not interconnect easily with more conventional strip-line circuits in which the strip is parallel to the ground planes. Also, current tends to concentrate at the thin edges of the strips in this construction, causing higher losses.

It is also possible to use thick bars for strips in order to achieve sufficient inter-strip capacitance, but this

* Received by the PGMTT, June 2, 1961; revised manuscript received, July 7, 1961. This work was supported by the U. S. Army Signal Research and Development Laboratory, Fort Monmouth, N. J., as part of Contract DA 36-039 SC-74862, Sub-Task 3-26-01-701, DA Project 3-26-01-000.

† Electromagnetics Laboratory, Stanford Research Institute, Menlo Park, Calif.